Iranian Journal of Materials Science and Engineering, Vol. 17, Number 4, December 2020
RESEARCH PAPER

The Effects of Contact Paste Type and Electric Field on Physical Properties of Zirconia Bodies Made by Flash Sintering Method: Modeling via Response Surface Methodology

H. Mohebbi[1, 2] and S. M. Mirkazemi[1*]

** mirkazemi@iust.ac.ir*

Received: June 2020 Revised: August 2020 Accepted: September 2020

[1] Department of Metallurgy and Materials Science, Iran University of Science and Technology, Tehran, Iran
[2] Renewable Energy Department, Niroo Research Institute (NRI), Tehran, Iran

DOI: 10.22068/ijmse.17.4.93

Abstract: *Flash sintering of 8 mol % yttria-stabilized zirconia (8YSZ) as solid oxide fuel cell (SOFC) electrolyte is studied. The relation between relative density, shrinkage, sample temperature during the flash, and incubation time, with the electric field strength, current density, as well as contact paste, are modeled by response surface methodology (RSM). The electric field strength and current density varied from 50 to 400 V.cm-1 and 50 to 200 mA.mm^{-2}, respectively. Also, platinum (Pt) and lanthanum strontium manganite (LSM) used as contact paste. Results show that using LSM paste lead to higher density and more shrinkage compare with Pt paste. In contrary, the electric field strength has no significant effect on density and shrinkage. However, a minimum electric field strength equal to 80 V.cm^{-1} is necessary for flash onset. As the field increases, the incubation time decreases dramatically. Compare with samples with LSM paste, samples with Pt contact paste reach a higher temperature during the flash. Flash sintered 8YSZ shows the mean grain size of 0.3 μm, which is about half of the conventionally sintered 8YSZ. Electrochemical Impedance Spectroscopy reveals despite lower mean grain size, the resistivity of flash sintered 8YSZ is lower than conventionally sintered 8YSZ.*

Keywords: *8YSZ, flash sintering, contact paste, platinum (Pt), lanthanum strontium manganite (LSM), current density, electric field strength, Response Surface Method.*

1. INTRODUCTION

8YSZ (zirconia stabilized with 8% mol yttria) is the most commonly used electrolyte in solid oxide fuel cells (SOFCs). The excellent ionic conductivity at high-temperature, superior stability in both reducing and oxidizing atmosphere, and compatible thermal expansion with other SOFC components have made it the most proper electrolyte material [1, 2]. Sintering of 8YSZ by conventional methods performs at elevated temperature (above 1400 ˚C) with long dwelling time (4-6 hours) [3, 4], which causes unfavorable reactions and transformations, composition changes, long process time, and more process cost [5]. So, various efforts have been done to sinter 8YSZ at lower temperatures and shorter time. Up to now, microwave sintering, spark plasma sintering, hot pressing, and high-pressure sintering [4–8] have been applied.

Flash sintering (FS) as an innovative sintering method has recieved more interest since its first report [9]. Its capability to sinter materials in a short time and low temperature made it a promising method for the sintering of a vast range of materials. The process involves applying an electric field to a sample placed in an electric furnace. The sintering onset is accompanied by a non-linear increase in conductivity, which results in a power surge and consequently, ultra-rapid sintering. Thus far, various ceramics such as oxygen ionic ceramics [9-12], protonic conductors [13], and electronic conductors [14-16] have been successfully densified using the flash-sintering technique. Compared to conventional sintering processes, flash sintering has several advantages. The boldest one is the energy saving due to the drastic reduction of time and temperature needed for ceramic densification. The densification time for flash sintering is typically a few seconds, whereas some hours are needed for conventional processes [9-16]. The low temperatures as well as the very short time in flash sintering, can simplify manufacturing processes, reduce capital costs, and mitigate undesirable reactions [10]. Out of equilibrium nature of flash sintering which arises from high heating rates and short sintering times, making it a proper method to sinter metastable materials and avoid undesired phase transitions [17, 18]. The main limitation of the flash sintering is “hot spots” [19, 20], which is related to the formation

[DOI: 10.22068/ijmse.17.4.93]

of preferential paths for current passage, especially in wide samples. Some technical solutions have been developed to avoid hot spot formation during flash sintering [21]. Local contamination with contact pastes, which are used to improve the electrical contact between electrodes and the samples, is another limitation of flash sintering. Herein, efforts led to the development of contactless-flash sintering [22].

Yttria stabilized zirconia (YSZ) was the first and one of the most considered materials sintered by FS. A widespread range of electric field strength and current density have been used by various researchers to flash sinter stabilized zirconia but the effects of process parameters on properties of flash sintered YSZ are adequately unstudied, and the optimum condition has not been reported yet. Cologna et al. [10] performed flash sintering in a non-isothermally manner and achieved a density of 96 %. Downs et al. [11] reported that full sintering did not occur with a DC field density of 2250 $V.cm^{-1}$ at 390 °C. Steil et al. [23] achieved 89 % of theoretical density with an AC electric field strength of 190 $V.cm^{-1}$ and the current density of 60 $mA.mm^{-2}$ at 800 °C. Baraki et al. [24] achieved a density of 79 % with an AC flash sintering at 1150 °C for 3min whose applied electric field strength and current density were 40 $V.cm^{-1}$ and 65 $mA.mm^{-2}$, respectively.

The design of experiments (DOE) involves developing a set of experiments to study the effect of experimental variables on a phenomenon so that maximum information can be extracted with a limited number of experiments [25]. Among various DOE methods, response surface methodology (RSM) helps to quantify the relationships between one or more measured characteristics and the vital input factors to develop, improve, and optimize a process. Where several variables potentially influence the performance or characteristic of the product or process, RSM is very beneficial. The developed model between response and independent variables by RSM can be used to investigate the relationship between independent variables and response to predict future observations within the design range [26].

In this study, the Response surface method was used to model the flash sintering of an 8YSZ body by correlating parameters like electric field strength, current density and contact paste to relative density, sample temperature, shrinkage, and incubation time. Established response surfaces were used to analyze the process, and the optimum sample was analyzed by scanning electron microscopy (SEM), electrochemical impedance spectroscopy (EIS) and compared with conventionally sintered one.

2. EXPERIMENTAL PROCEDURE

8YSZ slurry was produced by mixing commercial 8YSZ powder (Tosoh Corp., Japan) with ethanol and toluene as the solvent, polyvinyl butyral (PVB) as the binder, benzyl butyl phthalate (BBP) as the plasticizer, and terpineol (MERCK) as the dispersant in a ball mill. The composition of the slurry is listed in table 1. The slurry was tape cast with a house-made tape caster to the tapes with 90 μm thickness. The taps cut to the appropriate dimension and laminated to a thickness of 300 μm. The samples were cut to a dog-bone shaped sample and heated to 1000 ˚C for binder burnout [27]. Each end of the specimens was painted with a contact paste. After curing the contact pastes, the specimen were suspended in a tube furnace with a pair of platinum wire as electrodes. The furnace was heated up from room temperature to 800 ˚C at the constant heating rate of 10 $˚C.min^{-1}$. Before performing flash sintering, the samples were held at 800 ˚C for 30 min to ensure temperature uniformity. DC field was applied to the sample with a power generator (PAYA PAJOOHESH PARS, EPS Universal), and voltage, and the passing current was monitored by a digital multimeter (GW-INSTEK GDM-397). Samples were held for 30 seconds at the flash condition. The process was recorded by a digital camera equipped with an IR filter. For comparison, a sample was conventionally sintered in an electric furnace at 1400 ˚C for 4 hours with the increasing temperature rate of 5 $˚C.min^{-1}$.

The temperature of samples during flash was measured by using equation 1 according to the relation proposed by Amher et al. [28] for the conductivity of 8YSZ:

$$\frac{J_{flash}}{E_{flash}} T_{flash} = \left(\frac{1}{52.7\times10^{3}\times e^{-0.568/kT}\,flash} + \frac{1}{1.35\times10^{7}\times e^{-1.096/kT}\,flash} \right)^{-1} \qquad (1)$$

[DOI: 10.22068/ijmse.17.4.93]

Where J_{flash} is current density in flashpoint, E_{flash} is electric field strength in flashpoint, and T_{flash} is sample temperature in flashpoint.
The relative density of samples was measured by the Archimedes method. Shrinkage of samples was measured by using the recorded image before and after flash sintering. The microstructure was characterized by scanning electron microscopy (TESCAN-VEGA II). Electrochemical impedance spectroscopy was used to measure the conductivity of flash sintered 8YSZ at 800 ˚C with a 10 mV AC signal in the frequency of 10 mHz to 1MHz.

Table 1. Slurry composition.

Material	rule	company	Weight percent
8YSZ	Solid powder	Tosoh	51
Ethanol	Solvent	Merck	21
Toluene	Solvent	Merck	17
Terpineol	Dispersant	Merck	1
Benzyl butyl phthalate	Plasticizer	Sigma Aldrich	5
Polyvinyl butyral	Binder	Sigma Aldrich	5

To investigate the process parameter, the Design of experiments/response surface methodology was used. Design-Expert software was used to design the experiments and analyze the data. Electric field strength, current density, and the type of contact paste were selected as independent variables, and by using central composite design the values of parameters were determined. The limits of variables are listed in table 2. These limits were chosen according to power supply limits. Lanthanum strontium manganite and platinum pastes were used as the contact paste. The values of flash sintering parameters for 2 numeric factors (electric field strength and current density) and 1 categoric factor (contact paste) with 5 replication for the center point are listed in table 3. Relative density, sample temperature, shrinkage, and incubation time were chosen as responses.

Table 2. Limits of variables.

variable	unit	Lower limits	Upper limits
Electric field strength	$V.cm^{-1}$	50	400
Current intensity	$mA.mm^{-2}$	50	200

3. RESULTS AND DISCUSSION

3.1. Flash Sintering Phenomenon

At 800 ˚C with electric field strength equal to 50 $V.cm^{-1}$, no flash happened even after 10 minutes, i.e. a minimum electric field strength is necessary for flash happening. By increasing electric field strength stepwise, the flash phenomena happened in 80 $V.cm^{-1}$. By connecting the sample to the power supply, it showed an incubation time depended on the applied electric field strength (Figure 1). After incubation time, the current passing the sample started to increase, the electric field strength dropped, and an intensely bright light was emitted by the sample, which was accompanied by an obvious shrinkage. After this stage, a constant current equal to the current limit set on the power supply passed the specimen. These three stages typically are shown in Fig. 1.

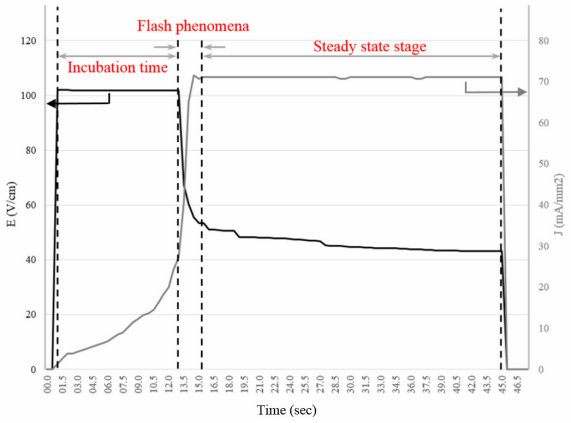

Fig. 1. Typical Electric field strength and current density passing the sample versus time during flash sintering.

3.2. RSM Model Establishment

By using central composite design, 13 sets of experiments were established for each contact paste (four axial points, four factorial points and, five replications for the central point). Points and the order of the experiments were determined by the Design-Expert software. Relative density, sample temperature, shrinkage, and incubation time were measured for each sample. Table 3 shows the design matrix and the corresponding responses.
The data were analyzed by software, and the best-fitting model was chosen for each response. The ANOVA data of relative density, sample temperature, shrinkage, and incubation time are shown in tables 4 to 7, respectively. The ANOVA

[DOI: 10.22068/ijmse.17.4.93]

data, residual normal distribution diagrams, residual vs. prediction plots, and prediction vs. actual values of responses altogether suggested that models proposed for each response (table 8), are accurate and can be used to describe the relationship between flash sintering and process parameters. Predicted models are shown in Figures 2, 3, 5, and 6 graphically.

Table 3. Experimental condition and responses.

Designed points				Responses			
Run	Electric field strength ($V.cm^{-1}$)	Current density ($mA.mm^{-2}$)	Contact paste	Relative density (%)	Shrinkage (%)	Temperature (°C)	Incubation time (sec)
1	225	125	LSM	85.0373	14.6627	1088.5	1.52
2	225	125	Pt	79.2615	9.720786	1155	1
3	225	200	Pt	96.9268	14.44115	1337.9	1.4
4	225	50	Pt	73.2018	1.648352	917.2	1.62
5	348	70	Pt	67.6743	5.2145	957.02	0.44
6	225	50	LSM	71.7076	6.774194	906.4	1.36
7	101	176	LSM	93.9597	20.9362	1238.19	13
8	225	125	Pt	77.5336	8.09674	1194.22	1
9	400	125	Pt	81.85	11.51151	1200.25	0.5
10	225	200	LSM	96.3785	17.31602	1291	1.38
11	225	125	Pt	73.6141	4.495504	1141.3	0.9
12	348	176	LSM	93.1658	15.22989	1372.35	0.46
13	400	125	LSM	93.075	15.8757	1194	0.24
14	101	70	Pt	76.1629	6.387435	1008.24	14.6
15	50	125	Pt	-	-	-	-
16	225	125	LSM	90.2545	15.75177	1092.38	0.83
17	101	176	Pt	86.787	14.12602	1308.4	16.08
18	225	125	LSM	89.1058	15.5894	1085.36	1.52
19	225	125	LSM	90.263	15.3456	1090.01	1.52
20	348	176	Pt	91.3332	14.0121	1483.34	0.52
21	225	125	LSM	83.3197	13.6154	1094.52	0.42
22	225	125	Pt	75.2192	10.63395	1169.77	1.54
23	348	70	LSM	69.7249	9.05307	989.01	0.66
24	101	70	LSM	73.9693	9.381663	993.58	13
25	50	125	LSM	-	-	-	-
26	225	125	Pt	79.5657	10.54217	1194.22	1.34

Table 4. ANOVA analysis for relative density (linear model).

Source	Sum of Squares	df	Mean Squared	F value	p-value prob>F	
Model	1.307E+006	2	6.536E+005	45.54	<0.0001	Significant
B- Current density	1.126E+006	1	1.126E+006	78.46	<0.0001	
C-contact paste	1.810E+005	1	1.810E+005	12.61	0.0019	
Residual	3.014E+005	21	14352.16			
Lack of fit	2.765E+005	19	14553.50	1.17	0.5589	Not significant
Pure Error	24878.81	2	12439.40			
Cor Total	1.609E+006	23				

[DOI: 10.22068/ijmse.17.4.93]

Table 5. ANOVA analysis for sample temperature (2FI model).

Source	Sum of Squares	df	Mean Squared	F value	p-value prob>F	
Model	8.105E+004	4	2.026E+004	84.57	<0.0001	Significant
A-electric field strength	2.170E+005	1	2.170E+005	9.06	0.0072	
B- Current density	7.399E+004	1	7.399E+004	308.83	<0.0001	
C-contact paste	2.590E+005	1	2.590E+005	10.81	0.0039	
AB	2.278E+005	1	2.278E+005	9.51	0.0061	
Residual	4.552E+005	19	2.396E+006			
Lack of fit	4.544E+005	17	2.673E+006	65.81	0.5101	Not significant
Pure Error	8.124E+008	2	4.062E+008			
Cor Total	8.560E+004	23				

Table 6. ANOVA analysis for shrinkage (linear model).

Source	Sum of Squares	df	Mean Squared	F value	p-value prob>F	
Model	1377.48	2	688.74	59.14	<0.0001	Significant
B- Current density	906.86	1	906.86	77.87	<0.0001	
C-contact paste	470.42	1	470.42	40.39	<0.0001	
Residual	224.58	21	11.65			
Lack of fit	236.12	19	12.43	2.94	0.2842	Not significant
Pure Error	8.46	2	4.23			
Cor Total	1622.06	23				

Table 7. ANOVA analysis for incubation time (quadratic model).

Source	Sum of Squares	df	Mean Squared	F value	p-value prob>F	
Model	3.26	2	1.63	216.03	<0.0001	Significant
A-electric field strength	3.24	1	3.24	428.51	<0.0001	
A^2	0.75	1	0.75	100.00	<0.0001	
Residual	0.16	21	7.550E-003			
Lack of fit	0.096	19	5.073E-03	0.16	0.9911	Not significant
Pure Error	0.062	2	0.031			
Cor Total	3.42	23				

Table 8. Predicted models for responses (J: current density, E: electric field strength).

response	Contact paste	model
Relative density (%)	LSM	$(RD)^{1.65}= +934.33948+5.0150\times J$
	Pt	$(RD)^{1.65}= +760.65307+5.0150\times J$
Sample temperature (˚C)	LSM	$T^{-0.09}= +0.54330+2.1428\times10^{-5}\times E-7.0993\times10^{-5}\times J-2.6\times10^{-7}\times E\times J$
	Pt	$T^{-0.09}= +0.54122+2.1428\times10^{-5}\times E-7.0993\times10^{-5}\times J-2.6\times10^{-7}\times E\times J$
Shrinkage (%)	LSM	$\Delta L^{1.18}= +5.19482+0.14335\times J$
	Pt	$\Delta L^{1.18}= -3.65975+0.14335\times J$
Incubation time (sec)	LSM and Pt	$(IT)^{0.25} =+3.10198-0.013496\times E+1.96362\times10^{-5}\times E^2$

3.3. Effect of Flash Sintering Parameter on Relative Density and Shrinkage

Response surfaces of relative density and shrinkage are shown in Figures 2 and 3, respectively. As can be seen, electric current density has a direct effect on relative density and shrinkage, but changing electric field strength does not affect. Also, contact paste has a

[DOI: 10.22068/ijmse.17.4.93]

significant effect on relative density as well as shrinkage; samples with LSM contact paste have higher relative density and shrinkage relative to those flash sintered with Pt contact paste. Nyquist plots of EIS spectra of the symmetrical 8YSZ disc painted with Pt and LSM are shown in Figure 4 with the corresponding equivalent circuit. LSM showed lower resistance against oxygen reduction in comparison with Pt (R2 in Table 9), and therefore, more oxygen ion would be generated using LSM. A portion of the current passed through the sample by oxygen ions; more oxygen ion led to more current passing the sample, resulting in more densification. Restriction of oxygen ion production on Pt increases the electrical resistance, and as shown in section 3-4 (Figure 5) will increase sample temperature during the flash sintering.

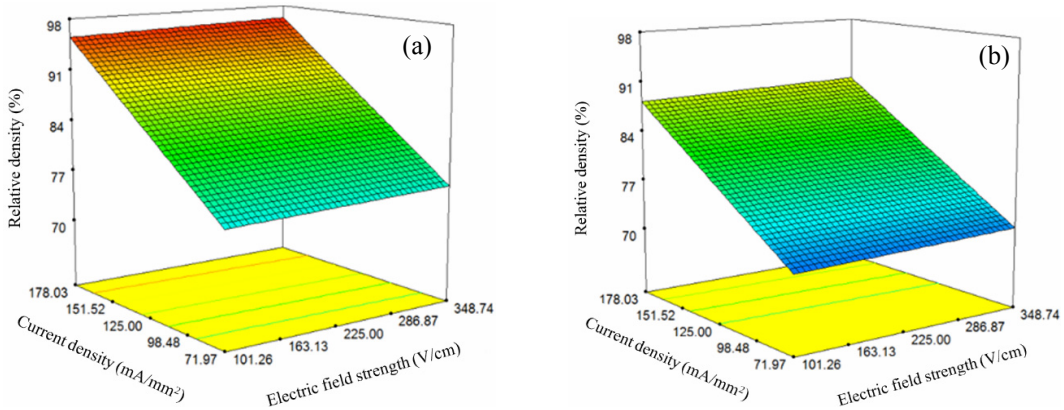

Fig. 2. Response surface of relative density a) LSM and b) Pt contact paste.

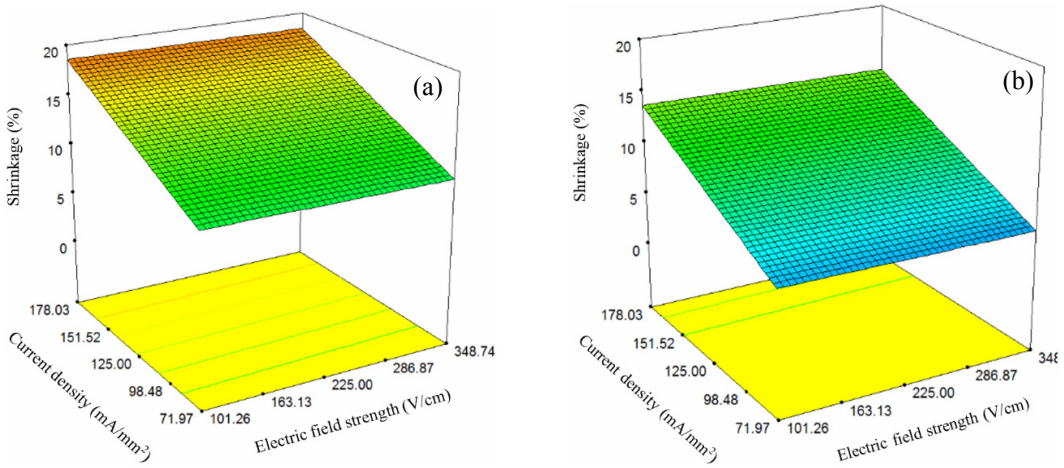

Fig. 3. Response surface of shrinkage a) LSM and b) Pt contact paste.

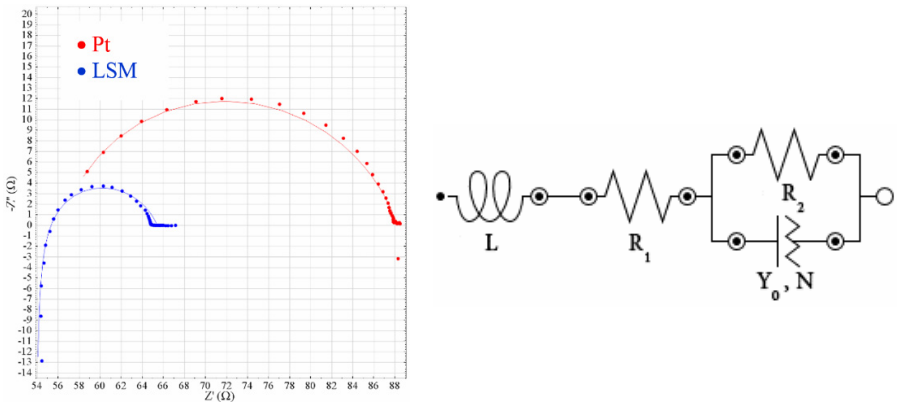

(a) (b)

Fig. 4. a) Nyquist plots of contact paste at 800 ˚C and b) Corresponding equivalent circuit.

[DOI: 10.22068/ijmse.17.4.93]

Table 9. The values of the equivalent circuit components.

Contact paste	L (μH)	R_1 (Ω)	R_2 (Ω)	Y_0 (μMho)	N
LSM	4.19	53.7	11.7	16.4	0.749
Pt	4.19	53.7	34.5	2.8	0.787

3.4. Effect of Flash Sintering Parameter on Sample Temperature

Fig. 5 shows the sample temperature surface versus current density, electric field strength, and contact paste. In contrast to relative density and shrinkage, the temperature of samples depended on both electric field strength and current density, and the higher the current density, the positive effect of electric field strength is more noticeable. Similar to shrinkage and relative density, contact paste has a significant effect on sample temperature but, here samples with Pt contact paste have attained a higher temperature during flash sintering in comparison with samples with LSM contact paste. The remarkable point is that the samples with higher flash temperature (Pt contact paste) have lower relative density compare with those with lower flash temperature (LSM contact paste). All of these results mean that Joule's heating lonely is not responsible for densification, and as noted earlier, the displacement of oxygen ions is also effective in the sintering process.

3.5. Effect of Flash Sintering Parameter on Incubation Time

With connecting the samples to the power supply, it takes a while for the flash phenomenon to happen, which is called incubation time [29]. Electric field strength has a very significant impact on incubation time (Fig. 6). Electric field strength equal to 50 $V.cm^{-1}$ led no flash happening. The observations showed that the minimum field strength required for the occurrence of the flash is 80 $V.cm^{-1}$. With increasing the electric field strength, the incubation time decreased drastically and reaches some milliseconds for E=400 $V.cm^{-1}$. Also, results showed that current density and contact paste type do not affect incubation time (Table 8). This behavior is the same as nucleation and growth in phase transformations; here, the electric field strength is the driving force for nucleation mechanisms.

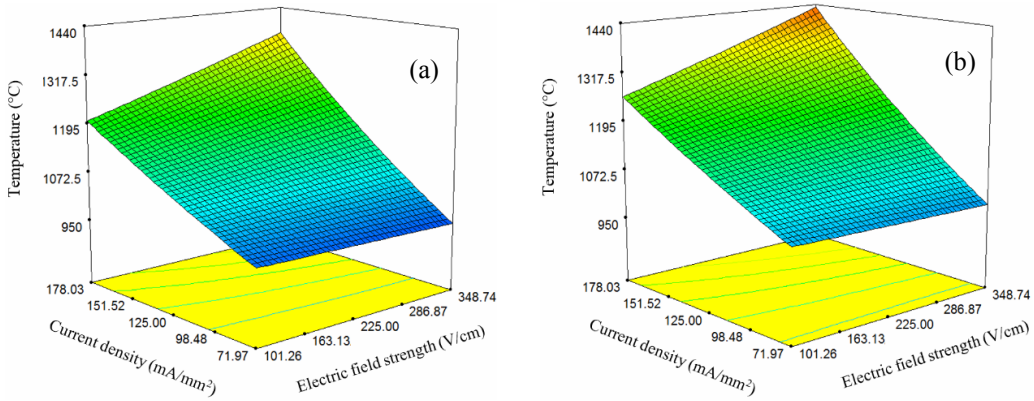

Fig. 5. Response surface of sample temperature a) LSM and b) Pt contact paste.

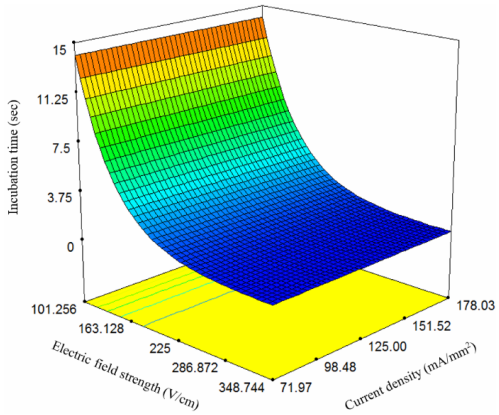

Fig. 6. Response surface of incubation time.

[DOI: 10.22068/ijmse.17.4.93]

3.6. Microstructure and Electrical Properties of Flash Sintered 8YSZ

Figure 7 shows the microstructure of the 8YSZ that flash sintered at 800 ˚C for 30 seconds (J=200 mA.mm^{-2} and E=100 V.cm^{-1}), and 8YSZ conventionally sintered at 1400 ˚C for 4 hours. The relative density of flash sintered 8YSZ was 97.3% and seems to be almost completely densified. The mean grain size was 0.3 µm and 0.75 µm for flash sintered and conventionally sintered 8YSZ, respectively. Fig. 8 shows EIS data of flash sintered 8YSZ at 800 ˚C. For comparison, the EIS spectrum of the conventionally sintered 8YSZ is showed in Fig. 8 (black-spectrum). The total electrolyte resistance (sum of bulk resistance and grain boundary resistance) is calculated from the intersection of the diagram with the real axis at high frequencies [28]. Flash sintered 8YSZ has lower resistance in comparison with conventionally sintered one. It is well-known that grain boundaries are blocking sites for ion conduction [30], and materials with small grain sizes have higher resistance in comparison with materials with large grain sizes. But in the present study, flash sintered 8YSZ with a small grain size has lower resistance. The formation of defect-enriched phases far from equilibrium has been reported in flash sintered materials [31, 32]; consequently, it seems that the flash sintering process has been changed the characteristic of grains and improve their conductivity by increasing oxygen vacancies in 8YSZ. Although this hypothesis needs to be studied in more detail.

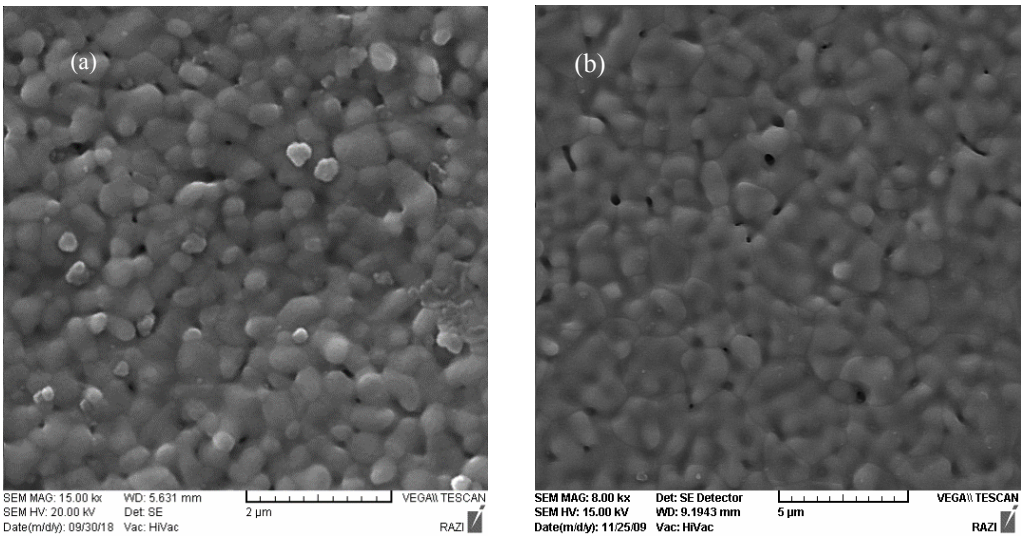

Fig. 7. SEM micrograph of a) flash sintered and b) conventionally sintered 8YSZ.

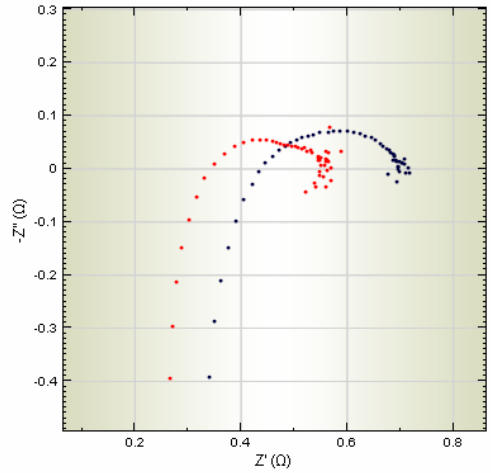

Fig. 8. EIS spectra of flash sintered (red) and conventionally sintered (black) 8YSZ.

[DOI: 10.22068/ijmse.17.4.93]

4. CONCLUSION

RSM methodology has been used to analyze the 8YSZ flash sintering process. Conclusions can be summarized as follows:

1. The relationship between the flash sintering parameter (electric field strength, current density, and contact paste) and relative density, shrinkage, sample temperature, and incubation time was established.
2. Electric field strength did not affect the densification of 8YSZ, but a minimum electric field strength was needed for flash happening. In the present study, this critical electric field strength was 80 $V.cm^{-1}$. Results showed incubation time strongly influenced by the electric field strength and decreased drastically with electric field strength increases.
3. Current density had a positive effect on relative density, shrinkage, and sample temperature, but the incubation time was independent of current density.
4. Contact paste affects the properties of sintered samples by influencing the amount of oxygen ion produced. The more oxygen ion led to more current passing the specimen and higher density. Conversely, the lower the amount of oxygen ion, the higher the resistance against current passing, resulting in a higher flash temperature.
5. The results showed that only joule's heating was not responsible for densification. Although samples with Pt contact paste reached a higher temperature during flash sintering, they had lower density compared with LSM contact paste samples.
6. Flash sintered 8YSZ had smaller grain size and lower overall resistance in comparison with conventionally sintered one. Contrary to conventional sintering data here, a decrease in grain size had led to lower resistance. It seems that flash sintering changes the characteristic of materials. This matter needs to be studied in more detail.
7. According to the results obtained in this study, the optimum conditions for 8YSZ flash sintering at 800 °C are LSM contact paste, the current density of 200 mA/mm^2, and the electric field strength of 100 V/cm.

ACKNOWLEDGMENT

This research was supported by Iran national science foundation (INSF).

REFERENCES

1. Mahato, N., Banerjee, A., Gupta, A., Omar, S., Balani, K., "Progress in material selection for solid oxide fuel cell technology: A review", Progress in Materials Science, 2015, 72, 141-337.
2. Steele, B.C.H., Heinzel, A., "Materials for fuel-cell technologies", Nature, 2001, 414, 345–352.
3. Flegler, A.J., Burye, T.E., Yang, Q., Nicholasn, J. D., "Cubic yttria stabilized zirconia sintering additive impacts: A comparative study", Ceramics International, 2014, 40, 16323–16335.
4. Dahla, P., Kausa, I., Zhaob, Z., Johnssonb, M., Nygrenb, M., Wiika, K., Grandea, T., Einarsruda, M.A., "Densification and properties of zirconia prepared by three different sintering techniques", Ceramics International, 2007, 33, 1603–1610.
5. Kuang, X., Carotenuto, G., Nicolais, L., "A Review of Ceramic Sintering and Suggestions on Reducing Sintering Temperatures", Advanced Performance Materials, 1997, 4, 257–274.
6. Rajeswari, K., Suresh, M.B., Hareesh, U.S., Rao, Y.S., Das, D., Johnson, R., "Studies on ionic conductivity of stabilized zirconia ceramics (8YSZ) densified through conventional and non-conventional sintering methodologies", Ceram. Int., 2011, 37, 3557–3564.
7. Rajeswari, K., Suresh, M.B., Chakravarty, D., Das, D., Johnson, R., "Effect of nano-grain size on the ionic conductivity of spark plasma sintered 8YSZ electrolyte", Int. J. Hydrogen Energy, 2012, 37, 511–517.
8. Li, Q., Xia, T., Liu, X.D., Ma, X.F., Meng, J., Cao, X.Q., "Fast densification and electrical conductivity of yttria-stabilized zirconia nano-ceramics", Mater. Sci. Eng. B, 2007, 138, 78–83.
9. Cologna, M., Rashkova, B., Raj, R., "Flash sintering of nanograin zirconia in <5 s at 850 °C", J. Am. Ceram. Soc., 2010, 93, 3556–3559.

[DOI: 10.22068/ijmse.17.4.93]

10. Cologna, M., Prette, A. L. G., Raj, R., "Flash-Sintering of Cubic Yttria-Stabilized Zirconia at 750 ˚C for Possible Use in SOFC Manufacturing", J. Am. Ceram. Soc., 2011, 94, 316–319.
11. Downs, J. A., Sglavo, V. M., "Electric Field Assisted Sintering of Cubic Zirconia at 390°C", J. Am. Ceram. Soc., 2013, 96, 1342–1344.
12. Hao, X. M., Liu, Y. J., Wang, Z. H., Qiao, J. S., Sun, K. N., "A novel sintering method to obtain fully dense gadolinia doped ceria by applying a direct current", J. Power Sources, 2012, 210, 86–91.
13. Jiang, T. Z., Liu, Y. J., Wang, Z. H., Sun, W., Qiao, J. S., Sun, K. N., "An improved direct current sintering technique for proton conductor – $BaZr_{0.1}Ce_{0.7}Y_{0.1}Yb_{0.1}O_3$: The effect of direct current on sintering process", J. Power Sources, 2014, 248, 70–76.
14. Gaur, A., Sglavo, V. M., "Densification of $La_{0.6}Sr_{0.4}Co_{0.2}Fe_{0.8}O_3$ ceramic by flash sintering at temperature less than 100 ˚C", J. Mater. Sci., 2014, 49, 6321–6332.
15. G. Prette, A. L., Cologna, M., Sglavo, V., Raj, R., "Flash-sintering of Co_2MnO_4 spinel for solid oxide fuel cell applications", J. Power Sources, 2011, 196, 2061–2065.
16. Gaur, A., Sglavo, V. M., "Flash-sintering of $MnCo_2O_4$ and its relation to phase stability", J. Eur. Ceram. Soc., 2014, 34, 2391–2400.
17. Shomrat, N., Baltianski, S., Randall, C.A., Tsur, Y., "Flash sintering of potassium-niobate", J. Eur. Ceram. Soc., 2015, 35, 2209–2213.
18. Perez-Maqueda, L.A., Gil-Gonzalez, E., Perejon, A., Lebrun, J.M., Sanchez-Jimeneza, P., Raj, R., "Flash Sintering of highly insulating nanostructured phase-pure $BiFeO_3$", J. Am. Ceram. Soc., 2017, 100, 3365–3369.
19. Trombin, F., Raj, R., "Developing processing maps for implementing flash sintering into manufacture of white ware ceramics", Am. Ceram. Soc. Bull., 2014, 93, 32–35.
20. "On the Hotspot Problem in Flash Sintering", Dong, Y., https://arxiv.org/ftp/arxiv/papers/1702/1702.05565.pdf
21. Sortino, E., Lebrun, J.M., Sansone, A., Raj, R., "Continuous flash sintering", J. Am. Ceram. Soc., 2018, 101, 1432–1440.
22. Saunders, T., Grasso, S., Reece, M.J., "Ultrafast-Contactless Flash Sintering using Plasma Electrodes", Sci. Rep., 2016, 6, 27222.
23. Steil, M.C., Marinha, D., Aman, Y., Gomes, J.R.C., Kleitz, M., "From conventional ac flash-sintering of YSZ to hyper-flash and double flash", J. Eur. Ceram. Soc., 2013, 33, 2093–2101.
24. Baraki, R., Schwarz, S., Guillon, O., "Effect of Electrical Field/Current on Sintering of Fully Stabilized Zirconia", J. Am. Ceram. Soc., 2012, 95, 75–78.
25. Mäkelä, M., "Experimental design and response surface methodology in energy applications: A tutorial review", Energy Conversion and Management, 2017,151, 630–640.
26. Myers, R.H., Montgomery, D.C., Anderson-cook, C.M., Response surface methodology: Process and Product Optimization Using Designed Experiments, Third Edition, John Wiley & Sons, Inc. 2009, 1-11
27. Ghobadzadeh, A. H., Mohebbi, H., Raoufi, A., Aslannejad, H., Davari, S., "Fabrication of Solid Oxide Fuel Cell Using the Dual Tape Casting Method", ECS Transactions, 2011, 35, 551-555.
28. Ahamer, C., Opitz, A.K., Rupp, G.M., Fleig, J., "Revisiting the Temperature Dependent Ionic Conductivity of Yttria Stabilized Zirconia (YSZ)", Journal of the Electrochemical Society, 2017, 164, F790-F803.
29. Yu, M., Grasso, S., Mckinnon, R., Saunders, T., Reece, M.J., "Review of flash sintering: materials, mechanisms and modelling", Advances in Applied Ceramics, 2017, 116, 24-60.
30. Zhu, B., "Solid oxide fuel cell (SOFC) technical challenges and solutions from nano-aspects", Int. J. Energy Res., 2009, 33, 1126–1137.
31. "Formation of defect-enriched phases far from equilibrium as a flash sintering mechanism", Jongmanns, M., Wolf, D. E., https://dc.engconfintl.org/efe_advanced materials_ii/80.
32. Jongmanns, M., Wolf, D.E., "Element-specific displacements in defect-enriched TiO_2: Indication of a flash sintering mechanism", J. Am. Ceram. Soc., 2020, 103, 589-596.

[DOI: 10.22068/ijmse.17.4.93]